



CLUSTERING BIFURCATION AND SPATIOTEMPORAL INTERMITTENCY IN RF-DRIVEN JOSEPHSON JUNCTION SERIES ARRAYS

FAGEN XIE

Institute of Theoretical Physics, Academia Sinica, Beijing 100080, China

HILDA A. CERDEIRA

*The Abdus Salam International Center for Theoretical Physics,
 P.O. Box 586, 34100 Trieste, Italy*

Received July 13, 1997; Revised December 16, 1997

We study the spatiotemporal dynamics of the underdamped Josephson junction series arrays (JJSA) which are globally coupled through a resistive shunting load and driven by an rf bias current. Clustering bifurcations are shown to appear. In particular, cluster-doubling induced period-doubling bifurcations and clustering induced spatiotemporal chaos are found. Furthermore, an interesting spatiotemporal intermittency is also found. These phenomena are closely related to the dynamics of the single cell.

The dynamics of globally chaotic systems has been of great interest in recent years. They arise naturally in studies of Josephson junctions arrays, multimode laser, charge-density wave, oscillatory neuronal system, and so on. Some rather surprising and novel features, such as clustering, splay state, collective behavior, and violation of the law of large numbers are revealed in these continuous and discrete globally coupled models [Benz *et al.*, 1990; Bhattacharya *et al.*, 1987; Chernikov & Schmidt, 1995; Domínguez *et al.*, 1991; Domínguez & Cerdeira, 1995; Eikmans & van Himbergen, 1991; Fisher, 1983; Free *et al.*, 1990; Hadley & Beasley, 1987; Hadley *et al.*, 1988; Hebboul & Garland, 1991; Kaneko, 1989; Kvale & Hebboul, 1991; Lee *et al.*, 1992; Middleton *et al.*, 1992; Strogatz & Mirollo, 1993; Tchiastikov, 1996; Tsang *et al.*, 1991; Tsang & Schwartz, 1992; Watanabe & Strogatz, 1993; Wiesenfeld *et al.*, 1996].

Being a paradigm for the study of nonlinear dynamical systems with many degrees of freedom, Josephson junction series arrays (JJSA) have been

a subject of active research. After scaling the parameters [Domínguez *et al.*, 1991], the dynamical equations of an underdamped JJSA shunted by a resistive load, and subject to an rf-bias current $I(t) = I_{dc} + I_{rf} \sin(\omega_{rf}t)$, [Hadley & Beasley, 1987; Hadley *et al.*, 1988; Tsang *et al.*, 1991; Tsang & Schwartz, 1992] are

$$\begin{aligned} \ddot{\phi}_i + g\dot{\phi}_i + \sin \phi_i + i_L &= i_{dc} + i_{rf} \sin(\Omega_{rf}\tau), \\ i_L = \sigma v(\tau) &= \frac{\sigma}{N} \sum_{j=1}^N g\dot{\phi}_j, \quad i = 1, \dots, N, \end{aligned} \quad (1)$$

where ϕ_i is the superconducting phase difference across the junction i . N is the total number of Josephson junctions or system size. Here, we use reduced units, with currents normalized by the critical current, $i = I/I_c$; time normalized by the plasma frequency $\omega_p t = \tau$, with $\omega_p = (2eI_c/\hbar C)^{1/2}$ and C the capacitance of the junctions; and voltages by rI_c , with r the shunt resistance of the junctions. i_L is the current flowing through the resistive load; $g = (\hbar/2eCr^2I_c)^{1/2} = \beta_c^{-1/2}$, with β_c the

McCumber parameter [McCumber, 1968; Stewart, 1968]; $v = V_{\text{total}}/N$ is the total voltage across the array per junction; $\sigma = rN/R$, with R the resistance of the shunting load, represents the strength of the global coupling in the array; and the normalized rf frequency is $\Omega_{\text{rf}} = \omega_{\text{rf}}/\omega_p$. Equation (1) exhibits rich spatiotemporal behavior, including phase locking, bifurcations, chaos, solitonic excitation, and pattern formation, breaking the law of large numbers and novel pseudo-Shapiro steps emerge in turbulence [Benz *et al.*, 1990; Domínguez *et al.*, 1991; Domínguez & Cerdeira, 1995; Eikmans & van Himbergen, 1991; Free *et al.*, 1990; Hebboul & Garland, 1991; Kvale & Hebboul, 1991; Lee *et al.*, 1992]. However, to the best of our knowledge, the mechanism of the transitions among these dynamical phases, specially the transition from coherence to turbulence, has never been discussed. In this paper we study the interesting spatiotemporal intermittency, clustering bifurcation and clustering induced spatiotemporal chaos in the system (1).

For a single cell (i.e. $N = 1$), the dynamical equation reduces to

$$\ddot{\phi} + \bar{g}\dot{\phi} + \sin \phi = i_{\text{dc}} + i_{\text{rf}} \sin(\Omega_{\text{rf}}\tau), \quad (2)$$

with $\bar{g} = (1 + \sigma)g$. It is well known that Eq. (2) can exhibit chaotic behavior in the underdamped regime, i.e. $\bar{g} < 1$ and $\Omega_{\text{rf}} < 1$ [Ben-Jacob *et al.*, 1982; Bhagavatula *et al.*, 1992; Huberman *et al.*, 1980; Iansiti *et al.*, 1984; Jensen *et al.*, 1984; Kautz & Monaco, 1985; Octavio & Raedi Nasser, 1984]. In Figs. 1(a) and 1(b) we show the bifurcation diagrams, for $\bar{g} = 0.2$, $\Omega_{\text{rf}} = 0.8$, as a function of i_{rf} and i_{dc} respectively. In Fig. 1(a) with $i_{\text{dc}} = 0.03$, the following points are to be remarked: First, the motion of the system (2) is period-1, then as i_{rf} increases to a critical value 0.662, in the system takes place a period-doubling bifurcation to period-2. Second, as i_{rf} continuously increases, the system undergoes a series of period-doubling bifurcation leading to a small scale region of chaos. At $i_{\text{rf}} \approx 0.832$, this chaotic attractor suddenly expands, and is replaced by a large scale chaotic motion. After the expanding transition the system acquires a rotating motion, and the time-averaged voltage becomes nonzero. The bifurcation diagram as a function of i_{dc} , with $i_{\text{rf}} = 0.61$, is shown in Fig. 1(b). The bifurcation behavior is essentially different from that of Fig. 1(a). As i_{dc} increases, the period-1 orbit first loses its stability, then a new period-2 solution arises via period-doubling bifurcation. The most

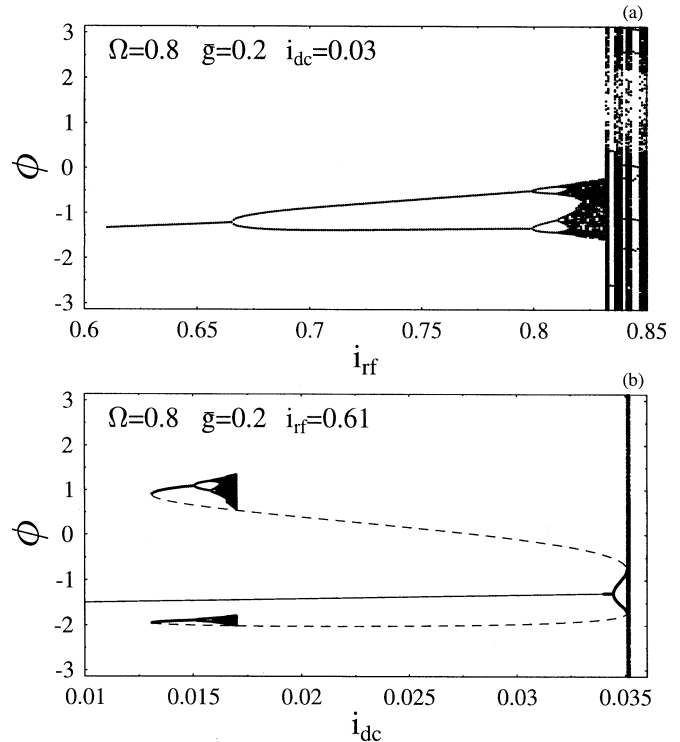


Fig. 1. Plots of ϕ at $t = nT$ ($T = 2\pi/\Omega_{\text{rf}}$), with n being large enough to exclude the transient process.

interesting and surprising point is that this period-doubling solution meets with an unstable period-2 orbit (the dashed lines), and they suddenly disappear via inverse tangent (saddle-node) bifurcation as i_{dc} reaches a critical value $i_{\text{dc}} \approx 0.035076$. Beyond this *threshold*, the behavior of the system is rotating and the motion is chaotic in a large scale region, and has the characteristic of type-I intermittency [Pomeau & Manneville, 1980]. In Fig. 1(b), it is clear that another period-2 orbit appears via tangent bifurcation for i_{dc} near zero. Increasing i_{dc} , this period-2 solution first bifurcates into a small region of chaos through a series of continuous period-doubling bifurcations, then this chaotic motion coincides with the unstable period-2 orbit, and suddenly disappears due to a boundary crisis [Grebogi *et al.*, 1983]. The two attractors form an interesting hysteresis phenomenon. In the following we investigate the complicated spatiotemporal dynamics in JJSA and how it originates from that of a single Josephson junction.

An important concept in a model for globally coupled systems is “clustering”. This means that even when the interaction between all elements is identical, the dynamics can break into different clusters, each of which consists of fully synchronized

elements. After the system falls in an attractor, we say that the elements i and j belong to the same cluster if $\phi_i \equiv \phi_j$ for all time. Therefore, the behavior of the whole system can be characterized by the number of clusters n_{cl} , and the number of elements of each cluster $(M_1, M_2, \dots, M_{n_{\text{cl}}})$ [Domínguez & Cerdeira, 1995; Kaneko, 1989].

The simplest attractor of the system (1) is the spatially homogeneous configuration, so called *coherent* state, i.e. $\phi_i(\tau) \equiv \phi(\tau)$, $n_{\text{cl}} = 1$, $M_1 = N$. Linearizing Eq. (1) around the $\phi(\tau)$ state

$$\delta\ddot{\phi}_i + g\delta\dot{\phi}_i + \cos\phi\delta\phi_i + \frac{\sigma}{N} \sum_{j=1}^N g\delta\dot{\phi}_j = 0, \quad i = 1, \dots, N. \quad (3)$$

Introducing the following coordinates defined by

$$X = \sum_{j=1}^N \delta\phi_j, \quad (4)$$

$$Y_k = \delta\phi_k - \delta\phi_{k+1}, \quad k = 1, \dots, N-1$$

After simple algebra, the critical stability boundaries of this coherent state are determined by the following set of linearizing equations:

$$\ddot{X} + \bar{g}\dot{X} + \cos\phi X = 0, \quad (5)$$

$$\ddot{Y}_k + g\dot{Y}_k + \cos\phi Y_k = 0, \quad k = 1, \dots, N-1.$$

The first equation in (5) is nothing but the equation obtained from linearizing the single cell case [Eq. (2)]. The second one characterizes the evolution of the difference of two cell perturbations. The interesting point here is that the second one has the same structure as the other except that it has g instead of the renormalized \bar{g} . Since the difference between the two is proportional to σ , the system recovers the single cell scenario when $\sigma = 0$. The critical boundaries of the coherent state in the σ versus i_{rf} parameter plane are shown in Fig. 2(a) with $\bar{g} = 0.2$, $i_{\text{dc}} = 0.03$ and $N = 128$. In the white region, the coherent state (motion in time may be regular and irregular) is *locally* stable, while in the shaded region, the coherent state loses its stability, and bifurcates to a multicluster state. As the coupling strength σ decreases to zero, the instability regions collapse to the discrete bifurcation points for a single cell ($\sigma = 0$). After the coherent state loses the stability, lots of multiclusters are created in the JJSA. A class of interesting states are multiclusters with a uniform distribution of junc-

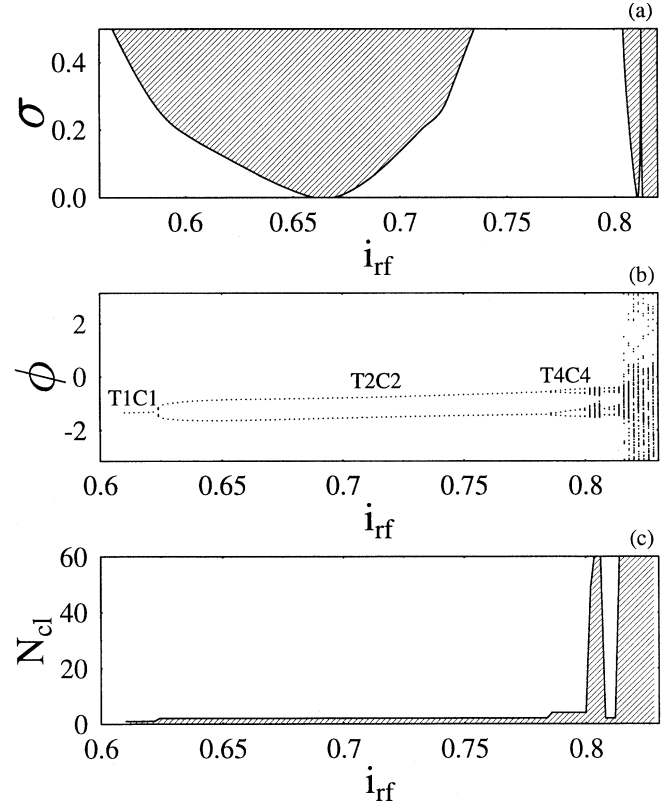


Fig. 2. (a) Bifurcation diagram for the homogeneous or coherent state in σ versus i_{rf} plane with $N = 128$. In the shaded region the coherent state is unstable due to the clustering bifurcation. (b) Bifurcation sequences plotted versus i_{rf} for $\bar{g} = 0.2$, $\Omega_{\text{rf}} = 0.8$, $i_{\text{dc}} = 0.03$, $\sigma = 0.1$ and $N = 128$. (c) The number of cluster, n_{cl} versus i_{rf} for the state of Fig. 2(b).

tions per cluster (i.e. $M_1 = \dots = M_{n_{\text{cl}}}$, with M_i , being the number of elements in the i th cluster), and each cluster may have the same motion except for uniformly distributed phase shifts. We focus on this kind of states, a period- m state with k clusters will be called TmCk state, and $N = k \times n$, $n = 1, 2, 3, \dots$. It often happens that $m = k$, then the dynamics of the TkCk state is reduced to

$$\ddot{\phi}(\tau) + g\dot{\phi}(\tau) + \sin\phi(\tau) + \frac{\sigma}{k} \sum_{j=1}^k g\dot{\phi}\left(\tau + \frac{2\pi}{\Omega_{\text{rf}}}j\right) = i_{\text{dc}} + i_{\text{rf}} \sin(\Omega_{\text{rf}}\tau). \quad (6)$$

To investigate the clustering bifurcations in JJSA with nonzero coupling, we show the asymptotic state of the system (1) in Fig. 2(b) as a function of i_{rf} with $\sigma = 0.1$, $N = 128$ and the other parameters equal to those of Fig. 1(a). However, the bifurcation diagram is essentially different from that of Fig. 1(a). The T1C1 (coherent) state first

undergoes a cluster-period-doubling bifurcation at $i_{rf} \approx 0.624$ to create a stable T2C2 state. By increasing i_{rf} , the state undergoes further cluster-period-doubling bifurcations leading to spatiotemporal chaos. Figure 2(b) is interesting due to the following novel features. First, we find a cluster-doubling induced period-doubling. The bifurcation point value is below the period-doubling condition for a single Josephson junction. Global coupling leads to cluster doubling at this parameter, which induces period doubling in time. Second, we find a cluster-doubling sequence 1-2-4 (and the induced period-doubling sequence). We expect that this clustering doubling cascade will proceed to a very large number of clusters and long periods. In our case this cascade is interrupted at $k = 4$ by a Hopf bifurcation, i.e. the modulus of another couple of complex eigenvalues is greater than *one*. Nevertheless, the tendency of cluster doubling bifurcations leading to spatiotemporal chaos can still be seen in Fig. 2(c), where we plot number of clusters versus i_{rf} for the state described in Fig. 2(b). Therefore, we conclude that spatiotemporal chaos is made possible by clusterization, and call it “clustering

induced spatiotemporal chaos”. Moreover, these cluster-doubling sequences grow from the period-doubling sequences of the single cell due to the nonzero global coupling. As σ decreases to zero, the clustering-doubling sequences is identified as the period-doubling sequence of the single cell. If the period-doubling sequence of the single cell is broken off, then the character of the clustering bifurcation in JJSA also changes suddenly. This can be clearly seen in Fig. 3(a) which shows the asymptotic state of the system (1) along the i_{dc} axis, with $\sigma = 0.6$ and the other parameters are the same as those of Fig. 1(b). The T1C1 state first undergoes a cluster-period-doubling bifurcation at $i_{dc} \approx 0.02087$ to create a stable T2C2 state. However, since the period-doubling period-2 solution in the single cell [see Fig. 1(b)] is destroyed by the inverse saddle-node bifurcation by increasing i_{dc} , the T2C2 state in the JJSA is suddenly destroyed by the spatiotemporal intermittency transition near $i_{dc} = 0.02143$. In Figs. 2(b) and 3(a), first we run Eqs. (1) to get the coherent (period-1) state from random initial conditions, then we compute Eqs. (1) by gradually increasing the parameter value (i_{dc} or i_{rf}) and by

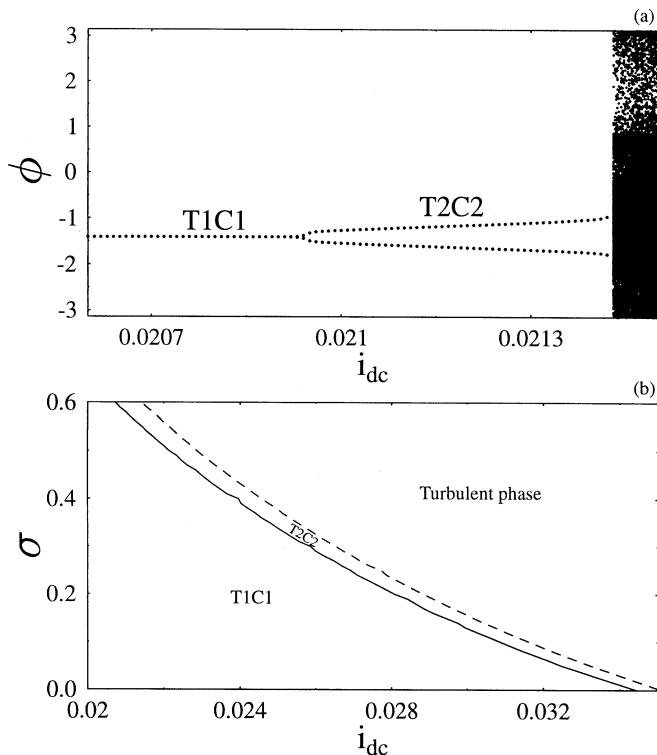


Fig. 3. (a) Bifurcation sequences plotted versus i_{dc} for $\bar{g} = 0.2$, $\Omega_{rf} = 0.8$, $i_{rf} = 0.61$, $\sigma = 0.6$ and $N = 128$. (b) The critical boundaries among the T1C1 state, the T2C2 state and the turbulent phase in i_{dc} - σ plane with the parameters of (a).

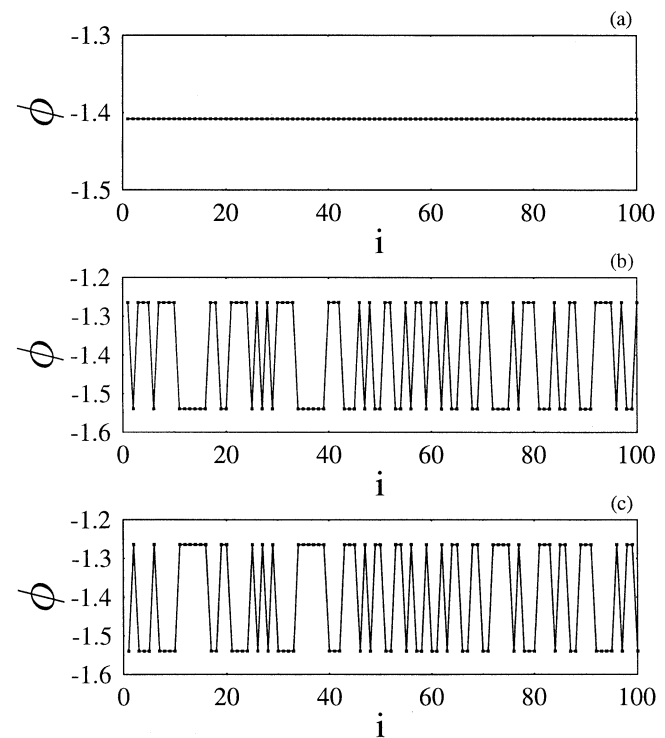


Fig. 4. Snapshot of the asymptotic solution of the system (1) after the transient process for $\bar{g} = 0.2$, $i_{rf} = 0.61$, $\Omega_{rf} = 0.8$, $\sigma = 0.6$, and $N = 100$. (a) $i_{dc} = 0.0206$, (b) and (c) are two successive snapshots for $i_{dc} = 0.0210$.

using the final state for the previous parameter value as the initial state for the new parameter value, in this way we can surely get clusters with a uniform distribution of cells for all cluster-doubling cascades. Figure 3(b) shows the phase diagram among T1C1 state, T2C2 state and the turbulent phase in the σ versus i_{dc} plane. The two critical transition curves in Fig. 3(b) are obtained by the numerical simulation of the system (1). It is clear that the regime of the T2C2 state is very narrow. Figures 4 shows the snapshots of ϕ for the T1C1 state and T2C2 state after a long transient process. The features of coherence and two-cluster are clearly observed in Figs. 4(a), and 4(b)–4(c), respectively. The most interesting phenomenon is that the system suddenly evolves to a very complicated rotating motion as i_{dc} is increased beyond a critical value ($i_{dc} \approx 0.02143$ for $\sigma = 0.6$), i.e. after the T2C2 state loses its stability. The system falls in a large $n_{cl} \sim N$ clusters motion with all M_j small. Figure 5 shows the space-time evolution after a very long and complicated transient process for $i_{dc} = 0.0215$ and $\sigma = 0.6$. The turbulent character of the motion is very clear. The evolution of ϕ_1 (the first junction) is displayed in Figs. 6(a) at the same parameters values as those of Fig. 5. The motion displays periodic behavior (2P) for a long time, it is suddenly interrupted by large

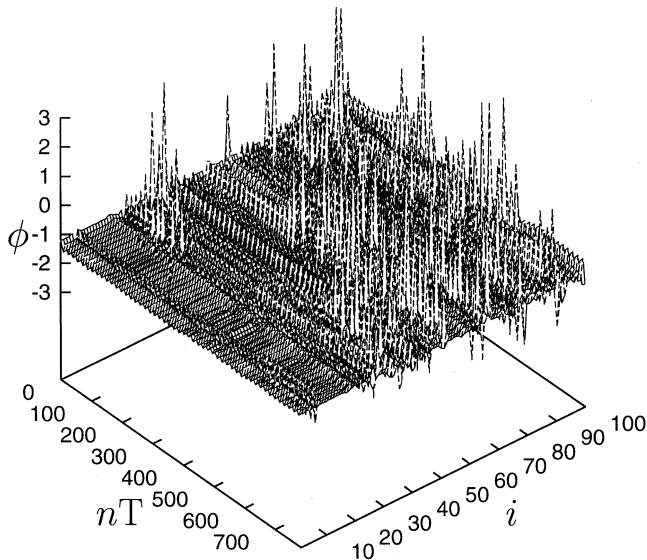


Fig. 5. The time-space evolution of the system (1) for $i_{dc} = 0.0215$ and the other parameters the same as those of Fig. 4. The plots are at $t = nT$ after some transient process, where T is the same as in Fig. 1. The features of turbulence are clearly observed.

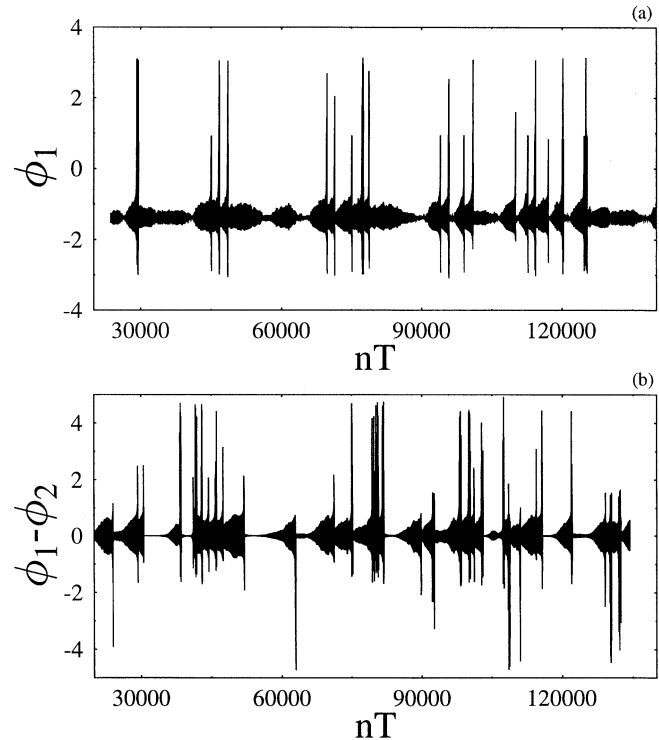


Fig. 6. The evolution of ϕ_1 and $\phi_1 - \phi_2$ with the same parameters as those of Fig. 5. The features of spatiotemporal intermittency are clear.

bursts and quickly resumes the periodic fashion. The similar features of the difference $\phi_1 - \phi_2$ are also displayed in Fig. 6(b). As i_{dc} is far from the critical value, more and more random large bursts take place more frequently. Although this behavior is similar to the characteristic of well-known intermittency, which were investigated in low-dimensional systems [Pomeau & Manneville, 1980], it is an essential type of spatiotemporal intermittency, which has not been found before in the rf-driven JJSA or other high dimensional globally chaotic systems. The above features do not depend on the specific cell and the number of cells. The spatial variable ($N \geq 2$), the dynamics of a single cell and the global coupling are of crucial importance for this interesting phenomenon.

In conclusion we analyzed the complex spatiotemporal dynamics of the rf-driven JJSA. Clustering bifurcation, clustering induced spatiotemporal chaos and spatiotemporal intermittency are shown to appear in these systems. The spatial variable, the dynamics of a single cell and the global coupling are of crucial importance for the existence of these interesting spatiotemporal phenomena.

References

- Ben-Jacob, E., Goldhirsh, I., Imry, Y. & Fishman, S. [1982] “Intermittent chaos in Josephson junctions,” *Phys. Rev. Lett.* **49**, 1599–1602.
- Benz, S. P., Rzchowski, M. S., Tinkham, M. & Lobb, C. J. [1990] “Fractional giant Shapiro steps and spatially correlated phase motion in 2D Josephson arrays,” *Phys. Rev. Lett.* **64**, 693–696.
- Bhagavatula, R., Ebner, C. & Jayaprakash, C. [1992] “Dynamics of capacitive Josephson junction arrays subjected to electromagnetic radiation,” *Phys. Rev.* **B45**, 4774–4787.
- Bhattacharya, S., Stokes, J. P., Higgins, M. J. & Klemm, R. A. [1987] “Temporal coherence in the sliding charge-density wave condensate,” *Phys. Rev. Lett.* **59**, 1849–1852.
- Chernikov, A. A. & Schmidt, G. [1995] “Conditions for synchronization in Josephson-junction arrays,” *Phys. Rev.* **E52**, 3415–3419.
- Domínguez, D., Jose, J. V., Karma, A. & Wiecko, C. [1991] “Novel axisymmetric coherent vortex state in arrays of Josephson junction far from equilibrium,” *Phys. Rev. Lett.* **67**, 2367–2370.
- Domínguez, D. & Cerdeira, H. A. [1995] “Spatiotemporal chaos in rf-driven Josephson-junction series arrays,” *Phys. Rev.* **B52**, 513–526.
- Eikmans, H. & van Himbergen, J. E. [1991] “Stability analysis of Shapiro steps in Josephson-junction arrays,” *Phys. Rev.* **B44**, 6937–6942.
- Fisher, D. S. [1983] “Threshold behavior of charge-density waves pinned by impurities,” *Phys. Rev. Lett.* **50**, 1486–1489.
- Free, J. U., Benz, S. P., Rzchowski, M. S., Tinkham, M., Lobb, C. J. & Octavio, M. [1990] “Dynamical simulations of fractional giant Shapiro steps in two-dimensional Josephson arrays,” *Phys. Rev.* **B41**, 7267–7269.
- Grebogi, C., Ott, E. & Yorke, J. A. [1983] “Crises, sudden changes in chaotic attractors and transient chaos,” *Physica* **D7**, 181–200.
- Hadley, P. & Beasley, M. R. [1987] “Dynamical states and stability of linear arrays of Josephson junctions,” *Appl. Phys. Lett.* **50**, 621–623.
- Hadley, P., Beasley, M. R. & Wiesenfeld, K. [1988] “Phase locking of Josephson junction arrays,” *Phys. Rev.* **B38**, 8712–8719.
- Hebboul, S. E. & Garland, J. C. [1991] “Radiofrequency spectral response of two-dimensional Josephson-junction arrays,” *Phys. Rev.* **B43**, 13703–13706.
- Huberman, B. A., Crutchfield, J. P. & Packard, N. H. [1980] “Noise phenomena in Josephson junctions,” *Appl. Phys. Lett.* **37**, 750–752.
- Iansiti, M., Hu, Q., Westervelt, R. M. & Tinkham, M. [1985] “Noise and chaos in a fractal basin boundary regime of a Josephson junction,” *Phys. Rev. Lett.* **55**, 746–749.
- Jensen, M. H., Bak, P. & Bohr, T. [1984] “Transition to chaos by interaction of resonances in dissipative systems. II. Josephson junctions, charged density waves and standard maps,” *Phys. Rev.* **A30**, 1970–1981.
- Kaneko, K. [1989] “Chaotic but regular Posi-Nega switch among coded attractors by cluster-size variation,” *Phys. Rev. Lett.* **63**, 219–223.
- Kautz, R. L. & Monaco, R. [1985] “Survey of chaos in the rf-biased Josephson junction,” *J. Appl. Phys.* **57**, 875–889.
- Kvale, M. & Hebboul, S. E. [1991] “Theory of Shapiro steps in Josephson junction arrays and their topology,” *Phys. Rev.* **B43**, 3720–3723.
- Lee, H. C., Newrock, R. S., Mast, D. B., Hebboul, S. E., Garland, J. C. & Loff, C. J. [1991] “Subharmonics Shapiro steps in Josephson junction arrays,” *Phys. Rev.* **B44**, 921–924.
- McCumber, D. E. [1968] “Effect of ac-impedance on dc voltage-current characteristics of superconductor weak-link junctions,” *J. Appl. Phys.* **39**, 3113–3118.
- Middleton, A. A., Biham, O., Littlewood, P. B. & Sibam, P. [1992] “Complete mode locking in models of charge-density waves,” *Phys. Rev. Lett.* **68**, 1586–1589.
- Octavio, M. & Readi Nasser, C. [1984] “Chaos in a dc-bias Josephson junction in the presence of microwave radiation,” *Phys. Rev.* **B30**, 1586–1588.
- Pomeau, Y. & Manneville, P. [1980] “Intermittent transition to turbulence in dissipative dynamical systems,” *Commun. Math. Phys.* **74**, 189–197.
- Stewart, W. C. [1968] “Current-voltage characteristics of Josephson junctions,” *Appl. Phys. Lett.* **12**, 277–279.
- Strogatz, S. E. & Mirollo, R. E. [1993] “Splay states in globally coupled Josephson arrays: Analytical prediction of Floquet multipliers,” *Phys. Rev.* **E47**, 220–227.
- Tchistiakov, V. [1996] “Detecting symmetry breaking bifurcations in the system describing the dynamics of coupled arrays of Josephson junctions,” *Physica* **D91**, 67–85.
- Tsang, K. Y., Strogatz, S. H. & Wiesenfeld, K. H. [1991] “Reversibility and noise sensitivity of Josephson arrays,” *Phys. Rev. Lett.* **66**, 1094–1097.
- Tsang, K. Y. & Schwartz, I. B. [1992] “Interhyperhedral diffusion in Josephson-junction arrays,” *Phys. Rev. Lett.* **68**, 2265–2268.
- Watanabe, S. & Strogatz, S. E. [1993] “Integrability of a globally coupled oscillation array,” *Phys. Rev. Lett.* **70**, 2391–2394.
- Wiesenfeld, K., Colet, P. & Strogatz, S. H. [1996] “Attractor crowding in oscillator arrays,” *Phys. Rev. Lett.* **76**, 404–407.